Spatial-temporal patterns of anthropogenic and biomass burning contributions on air pollution and mortality burden changes in India from 1995 to 2014

Bin Luo[1], Yuqiang Zhang[1], Tao Tang[2,3], Hongliang Zhang[4], Jianlin Hu[5], Jiangshan Mu[1], Wenxing Wang[1], Likun Xue[1]

[1]Environment Research Institute, Shandong University, Qingdao 266237, China
[2]School of the Environment, Yale University, New Haven, CT 06511, USA
[3]Institute of Atmospheric Physics, Chinese Academy of Sciences, Beijing 100029, China
[4]Department of Environmental Science and Engineering, Fudan University, Shanghai 200438, China
[5]Jiangsu Key Laboratory of Atmospheric Environment Monitoring and Pollution Control, Collaborative Innovation Center of Atmospheric Environment and Equipment Technology, Nanjing University of Information Science & Technology, Nanjing 210044, China

Correspondence to: Yuqiang Zhang (yuqiang.zhang@sdu.edu.cn), Likun Xue (xuelikun@sdu.edu.cn)

Abstract. Anthropogenic (ANTHRO) emissions and biomass burning (BB) are major contributors to ambient air pollution, with the latter playing a particularly dominant role in non-urban regions. India has experienced a dramatic deterioration in air quality over the past few decades, but no systematic assessment has been made to investigate the individual contributions of ANTHRO and BB emissions changes over the long term in India, extension to non-urban areas. In this study, we conduct a comprehensive analysis of the long-term trends of particulate matter with aerodynamic diameters < 2.5 μm ($PM_{2.5}$) and ozone (O_3) in India and their mortality burden changes from 1995 to 2014, using a state-of-the-art high-resolution global chemical transport model (CAM-chem). Our simulations reveal a substantial nationwide increase in annual mean $PM_{2.5}$ (6.71 μg m^{-3} $decade^{-1}$) and O_3 (7.08 ppbv $decade^{-1}$), with the Indo-Gangetic Plain (IGP) and eastern central India as hotspots for $PM_{2.5}$ and O_3 trend changes individually. Noteworthy substantial O_3 decreases were observed in the northern IGP, potentially linked to NO titration due to a surge in NOx emissions. Sensitivity analyses highlight ANTHRO emissions as primary contributors to rising $PM_{2.5}$ and O_3, while BB played a prominent role in winter and spring. In years with high BB activity, the contributions from BB emissions on both $PM_{2.5}$ and O_3 changes were comparable with or even exceeding ANTHRO emissions in specific areas. We further estimate that the elevated air pollutants were associated with increased premature mortality attributable to $PM_{2.5}$ and O_3, leading to 97.83 K and 73.91 K per decade. Despite a per capita decrease in the IGP region, the increased population offset its effectiveness.

1 Introduction

Air pollution is among the most detrimental environmental factors to human health. According to the World Health Organization (WHO) database, 99% of the global population lives in areas where air quality surpasses WHO guideline limits

(WHO: Air Pollution, World Health Organization, available at: https://www.who.int/health-topics/air-pollution#tab=tab_1, last access: 21 September 2024). The two most concerned pollutants, particulate matter with aerodynamic diameters < 2.5 μm ($PM_{2.5}$) and ozone (O_3), can cause significant damage to the human heart and lungs (Hoek et al., 2013; Hystad et al., 2013; Villeneuve et al., 2015), potentially leading to premature death when exposed over extended periods (Dedoussi et al., 2020; Fuller et al., 2022). The latest Global Burden Disease (GBD2019) study, a comprehensive research initiative that quantifies health loss due to diseases, injuries, and risk factors worldwide, estimated that exposure to air pollution, including both household and ambient pollution, led to 6.7 million premature deaths (95% confidence interval [CI], 5.9 to 7.5 million) worldwide in 2019 (GBD 2019 Risk Factors Collaborators., 2020). Thus, the urgency of dealing with air pollution has become one of the most pressing global challenges.

It is well-known that surface air pollution is usually unequally distributed in space, with higher levels in developing countries than in developed countries (GBD 2015 Risk Factors Collaborators., 2016). For example, India was ranked as the most polluted country in the world in 2021, with 63 of the world's 100 most polluted cities (IQAir: 2021 World Air Quality Report, available at: https://lib.icimod.org/record/35767/files/HimalDoc2022_2021WorldAirQualityReport.pdf?type=primary, last access: 21 September 2024). Previous modelling studies indicated that districts exceeding India's annual ambient standard of 40 $\mu g\ m^{-3}$ rose from 200 to 385 out of 640 from 1998 to 2020 (Guttikunda and Ka, 2022). The GBD2019 study estimated that premature deaths attributed to ambient $PM_{2.5}$ and O_3 pollution accounted for 10.4% (8.4-12.3) and 1.8% (0.9-2.7) of the total deaths in India in 2019, respectively, and the death rate per 100,000 people increased by 115.3% (28.3-344.4) and 139.2% (96.5-195.8) from 1990 to 2019, respectively (Pandey et al., 2021). However, the GBD2019 study did not separate the air quality changes due to various contribution factors, such as anthropogenic (ANTHRO) and biomass burning (BB). Meanwhile, the elevated chemical reaction rates in India, driven by intense sunlight and warm temperatures, create conditions conducive to ozone formation. Additionally, strong convection enhances the transport of ozone and its precursors, such as NOy, to higher altitudes, where the prolonged ozone lifetime promotes accumulation. This phenomenon positions India as a hotspot for ozone pollution, significantly impacting air quality in downwind regions (Zhang et al., 2016, 2021a).

As seen from the Community Emissions Data System (CEDS) inventory (Hoesly et al., 2018), the increasing trends of ANTHRO emissions of major air pollutants, such as nitrogen oxides (NOx), carbon monoxide (CO) and non-methane volatile organic compound (NMVOC), are significantly higher in India than those in other regions (Wang et al., 2022). Meanwhile, crop yields in India have significantly enhanced since the mid-1960s after the Green Revolution, contributing to increased BB emissions (Huang et al., 2022). The study showed that from 1950–51 to 2017–18, the crop residue burning in India increased from 18 million tonnes to 116 million tonnes in terms of total biomass burned (Venkatramanan et al., 2021). The frequency and intensity of forest fires in India have also increased in recent years due to persistent warmer temperatures and climate extremes (Vadrevu et al., 2019; Jain et al., 2021). These in turn could pose significant threats to ambient air quality and human health because large amounts of compounds are emitted into the atmosphere, namely carbon dioxide

65 (CO_2), NOx, particulate matter (PM), and other chemical species (Crutzen and Andreae, 1990; Carvalho et al., 2011; Lan et al., 2022; Miranda et al., 2005). Previous studies have utilized observational and satellite data to assess the impacts of ANTHRO and BB sources on air quality trends in some Indian cities (Gurjar et al., 2016; Vohra et al., 2022). Additionally, model simulations have been employed to analyze source contributions to air pollution (Conibear et al., 2018a, b). However, there remains a lack of comprehensive assessments regarding the impacts of long-term ANTHRO and BB emissions changes
70 on air quality, particularly in non-urban areas.

In this study, we aim to improve our understanding of the spatial-temporal distribution of major air pollutants, mainly surface $PM_{2.5}$ and O_3, and the related mortality burden in India from 1995-2014 using a state-of-the-art global chemistry transport model. In addition, the individual contributions of changes in ANTHRO and BB emissions were further separated to better understand the causes of worsening air quality and escalating health risks in India. The selected period encompasses
75 a dynamic phase of rapid changes in both ANTHRO and BB activities in India, thereby providing an ideal context for investigating their respective contributions to air pollution.

2 Methods

2.1 CAM-chem model configuration

We simulate surface $PM_{2.5}$ and O_3 concentrations over India between 1995 and 2014 using the global chemistry model
80 CAM-chem, which is based on version 6 of the Community Atmosphere Model (CAM6), the atmospheric component of the Community Earth System Model (CESM2), as detailed by Danabasoglu et al. (2020) and Emmons et al. (2020). Following Emmons et al. (2020), the original model is run at 1.25° (longitude) × 0.9° (latitude) horizontal resolution with 32 vertical levels reaching ~45 km. We configure the Model of Ozone and Related Chemical Tracers Tropospheric and Stratospheric (MOZART-TS1) chemistry mechanism with various complexity choices for tropospheric and stratospheric chemistry
85 (Emmons et al., 2020). The aerosol module adopts the four-mode version of the Modal Aerosol Model (MAM4), including sulfate, black carbon, primary organic matter, secondary organic aerosols, sea salt, and mineral dust. The first level of the model outputs is considered the surface level, and all the model outputs are then regridded to a finer resolution of 0.5° × 0.5° to match the grid-cell population and baseline mortality rates datasets in performing the health impact assessment.

Global historical ANTHRO emissions are adopted from CEDS (version 2017-05-18), which provides monthly
90 emissions of ANTHRO aerosol and precursor compounds at 0.5° × 0.5° from 1750 to 2014 and were used in the Coupled Model Intercomparison Project Phase 6 (CMIP6) experiments (Emmons et al., 2020; Hoesly et al., 2018). The ANTHRO emissions include eight sectors: agriculture; energy; industrial; transportation; residential, commercial, other; solvents production and application; waste and international shipping (Hoesly et al., 2018). The air pollutants from the CEDS inventory, especially the NMVOC, are then re-speciated to match the chemical species in the latest CESM2 model,
95 following the steps introduced by Emmons et al. (2020). Interpolation of the emission inventory from its original resolution

(0.5° × 0.5°) to the target model resolution (0.9° × 1.25°) before being input into the model. Global historical BB emissions are sourced from van Marle et al. (2017) at monthly temporal resolution and 0.5° native resolution, with all emissions occurring at the surface. Additionally, the biogenic emissions are calculated using the Model of Emissions of Gases and Aerosols from Nature (MEGAN v2.1). More emissions used are described in Emmons et al. (2020).

2.2 Numerical experiments designs

As described above, the standard simulation (BASE) is driven by year-to-year variability of ANTHRO and BB emissions from 1995 to 2014. To separate the contributions from these two emission sources, we then conduct two sensitivity simulations in which ANTHRO emissions (FixAN) and BB emissions (FixBB) are fixed at 1995 levels individually, while all other parameters are kept consistent with the BASE (Table 1). Subtracting the BASE from each sensitivity enables quantifying the influences of changes in ANTHRO and BB emissions on air quality and its associated health burden in India, respectively. We will discuss the air quality and mortality burden changes in six Indian regions based on meteorological conditions and aerosol variability (Fig. 1).

Table 1. Model simulations performed in this study

Simulation	Anthropogenic emissions	Biomass burning emissions
BASE	V	V
FixAN	1995	V
FixBB	V	1995

"V" indicates that particular input is subject to interannual variation in the simulation during the period 1995-2014, "FixAN" indicates that only global ANTHRO emissions are fixed to 1995 levels in the simulation. "FixBB" indicates that only global BB emissions are fixed to 1995 levels.

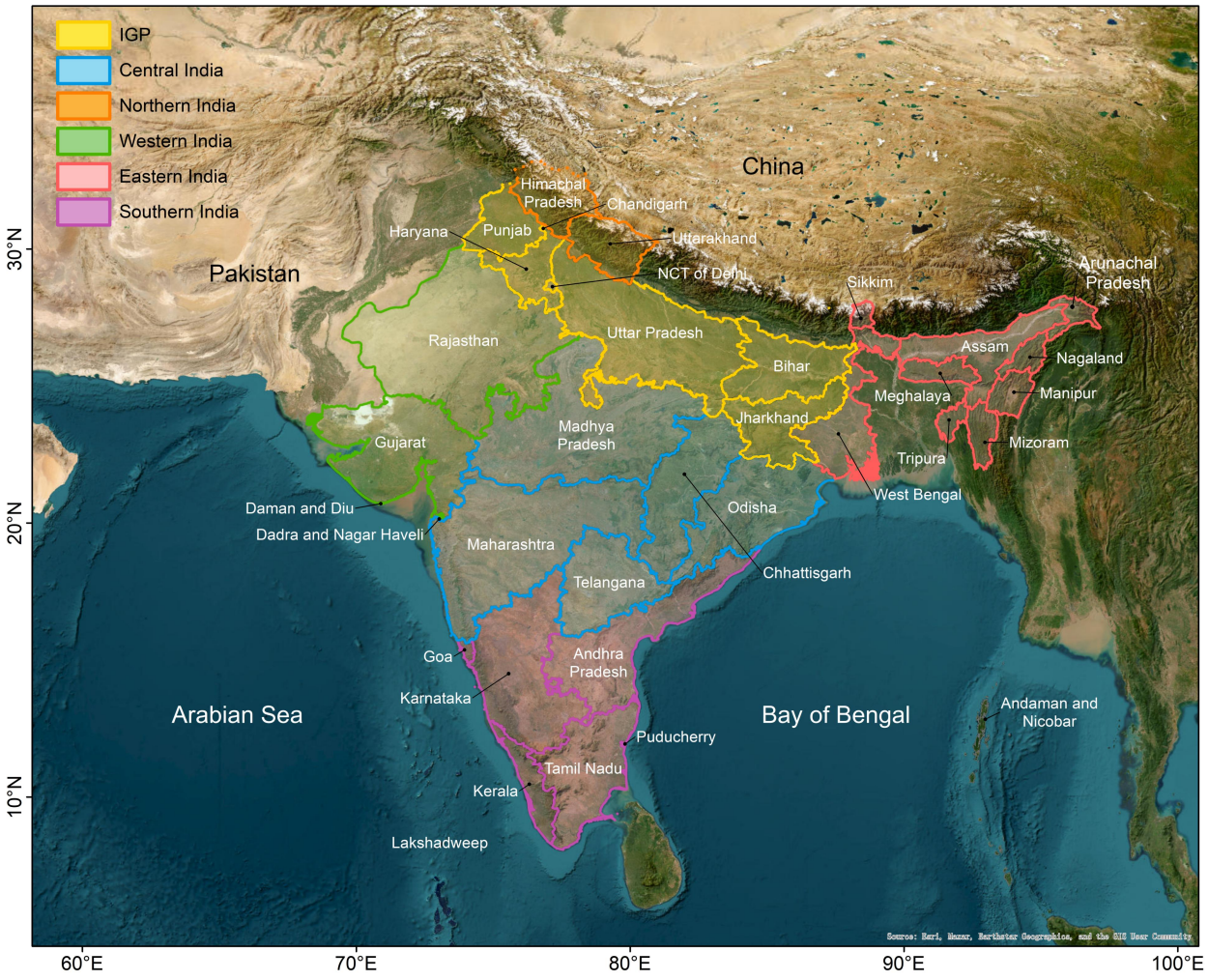

Figure 1. A map of India marked into six regions based on meteorological conditions and aerosol variability (adapted from David et al. 2018).

2.3 Trend estimation

In this study, we apply the Theil-Sen estimator (Theil, 1992; Sen, 1968) to calculate the magnitude of trends in surface $PM_{2.5}$ and O_3 concentrations and the attributed mortality burden spanning from 1995 to 2014. The Theil-Sen estimator is a robust non-parametric method for trend analysis based on the median slope, which is insensitive to outliers and highly competent in identifying the slope of non-normally distributed data, as described in eq 1. This method has been widely used

to analyse temporal trends in air pollutants that are always non-normally distributed (e.g., Munir et al., 2013; Sarkar et al., 2019; Vanem and Walker, 2013; Wan et al., 2023).

$$Slope = Median\frac{(x_i - x_j)}{(t_i - t_j)} \quad (1)$$

Where x_i and x_j represent the concentrations of either $PM_{2.5}$, O_3 or attributed premature mortality at the time t_i and t_j (i > j), respectively, for the same parameter. $Slope > 0$ indicates an increasing trend; $Slope < 0$ indicates a decreasing trend.

In complement to the Theil-Sen estimator, we use the nonparametric Mann-Kendall test to assess the significance of temporal trends within the data series (Zhang et al., 2022a, b). Both the Mann-Kendall test and Theil-Sen estimator require independence and randomness in the data, making them suitable for identifying monotonic trends. According to previous studies, p-value less than 0.05 is most commonly treated as the absolute threshold of statistical significance (Christiansen et al., 2020; Wang et al., 2021; Zhou et al., 2017). The above methods are completed by implementing a Python program with the package "pymannkendall", as detailed at https://pypi.org/project/pymannkendall/, last accessed on March 20, 2024.

2.4 Mortality burdens of surface $PM_{2.5}$ and O_3 in India

Based on an integrated exposure-response function utilized in the most recent GBD studies, we estimate the mortality burden associated with long-term exposure to ambient annual $PM_{2.5}$ and the O_3 season daily maximum 8-h mixing ratio (OSDMA8) in India spanning from 1995 to 2014, as described in eq 2.

$$\Delta Mort = y_0 \times AF \times pop = y_0 \times \left(\frac{RR - 1}{RR}\right) \times pop \quad (2)$$

Where $\Delta Mort$ refers to the annual mortality burden attributed to long-term $PM_{2.5}$ or O_3 exposure, and y_0 is the baseline mortality rate for a specific cause of disease. AF is the attributable fraction measuring the $PM_{2.5}$ or O_3 exposure attributable disease burden, which is represented by $\frac{RR-1}{RR}$ (RR refers to relative risk). pop represents the exposed population above the age of 25 for each grid cell in the domain.

Following our previous work (Zhang et al., 2021b), we obtain the baseline mortality rate (y_0) for each country and 5-year age group from 1995-2014 from the GBD2017 project (GBD 2017 Risk Factor Collaborators., 2018). The RR of long-term $PM_{2.5}$ exposure associated with mortality burden due to specific diseases was estimated using an integrated exposure-response model (IER) constructed by Burnett et al. (2014) and updated in GBD2017. The RR for long-term O_3 exposure is obtained from Turner et al. (2016) which indicated an RR of 1.12 (95% confidence interval (CI): 1.08, 1.16) for respiratory disease. The recent GBD2019 reported a relatively lower RR for the chronic obstructive pulmonary disease (COPD), a subcategory of respiratory disease (1.06, with 95% CI: 1.03, 1.10). To be comparable with the GBD2019 results, we also estimate the O_3-related mortality burden for the COPD in India during the same period. Population distribution with age

stratification data (pop) is retrieved from the GBD2017 with a horizontal resolution of 0.1°. The population-weighted (pop-weighted) average of specific air pollutants discussed in the results is calculated by weighting the population of all grid cells inside each administrative region or country. Additionally, we calculate mortality rates per capita (avoid deaths per 100,000 people) in each administrative region to exclude the influence of varying populations.

3 Results and discussion

3.1 CAM-chem evaluation

We perform a comprehensive model evaluation by comparing our simulated monthly concentrations from the BASE with multiple datasets, including ground-based observations in India, historical multi-model simulation from the CMIP6 project, and different versions of multi-year reanalysis data from the Atmospheric Composition Analysis Group (ACAG) at Washington University in St. Louis, hereinafter referred as 'Wustl Extracts' (van Donkelaar et al., 2021). We also compare our simulated $PM_{2.5}$ and O_3 with previously published studies in India using either global or regional chemical transport models (CTMs), as well as the concentration reported from the GBD2019. We select available ground-level $PM_{2.5}$ observations over India from previous studies (Latha and Badarinath, 2005; Panwar et al., 2013; Reddy et al., 2012; Saradhi et al., 2008; Tiwari et al., 2009, 2013), which were also collected by the ACAG. The locations of these sites are listed in Table S1. Figure S1 indicates that the model exhibits good performance in capturing seasonal variations of surface $PM_{2.5}$ observations, especially during the peak months, with correlation coefficients (R) ranging from 0.59 to 0.91. Two exceptions are Mumbai (with R of -0.16), where the model shows a contrasting trend for the seasonal $PM_{2.5}$ characteristics (Fig. S1b), and Mukteshwar (with R of 0.45). One possible explanation is the potential underestimation of emission inventories, especially during early periods for developing regions, such as India (McDuffie et al., 2020; Wang et al., 2022; Agarwal et al., 2024). For O_3, our model shows an even higher R when compared with the available surface observation sites in India from 1997 to 2011 (Fig. S2). Unlike the underestimations of surface $PM_{2.5}$ in India, the CAM-chem model tends to overestimate surface O_3, which is not very uncommon for global CTM and also frequently discussed in previous studies (Hou et al., 2023; Tilmes et al., 2015; Young et al., 2018; Zhang et al., 2021b). The overestimation is partly caused by the coarse resolution, which leads to diluted emissions of O_3 precursors and then simulated high O_3 production. Figure 2 compares our study with previous studies and other publicly available $PM_{2.5}$ and O_3 datasets, as detailed in Tables S2 and S3. The comparisons indicate our simulated results using the CAM-chem agree very well with previous studies for both $PM_{2.5}$ and O_3, based on either the various metrics, such as average O_3, pop-weighted average O_3 or OSDMA8, consistent with the findings within the multiple CMIP6 models (Turnock et al., 2020). Figure S3 further compares the long-term trend of annual surface $PM_{2.5}$ concentrations from 1998 to 2014 in the BASE and Wustl Extracts dataset. A consistent increasing trend is found in both datasets, with temporal R of 0.86 and lower estimations in our model. The model performs better in eastern India than in western India, with R usually larger than 0.9 and NMB lower than -25%. Similarly, compared to the simulated trend in our study with different versions of Wustl Extracts and the GBD2019, our simulated $PM_{2.5}$ concentration is lower,

and the simulated O_3 is higher (Fig. S4). The underestimation of the surface $PM_{2.5}$ is partly caused by the missing model representation of nitrate and ammonium (Ren et al., 2023) and the secondary organic aerosol (Liu et al., 2021).

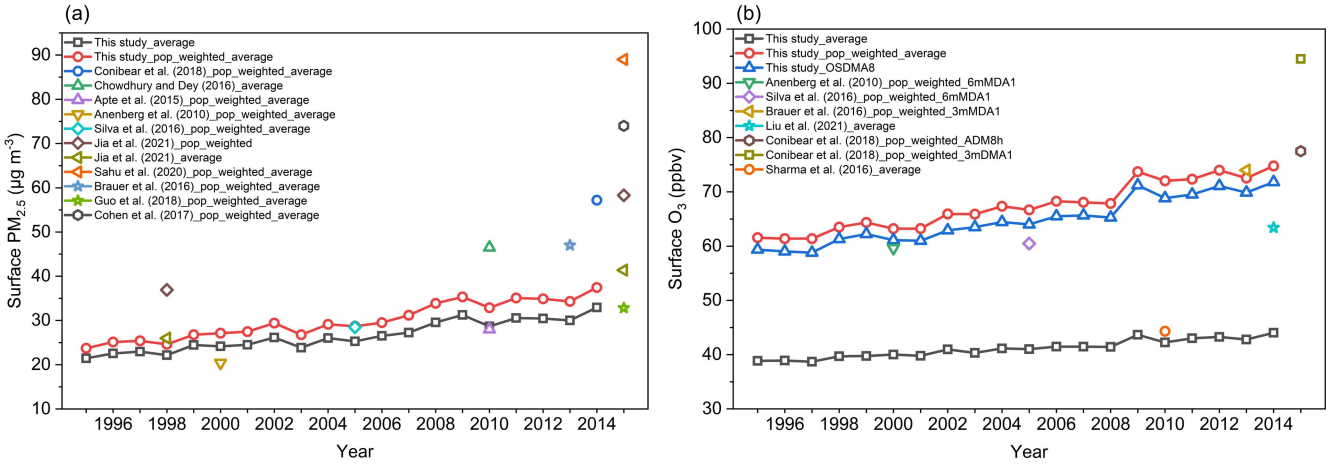

Figure 2. Comparison of annual $PM_{2.5}$ and O_3 concentrations in India with previous studies. Note that the metrics vary depending on the study.

3.2 Spatial and temporal distribution of air pollution changes in India from 1995 to 2014

3.2.1 Historical emissions in India from 1995 to 2014

We first assess the interannual variation of ANTHRO and BB emissions of CO, NOx, NMVOC, sulfur dioxide (SO_2), ammonia (NH_3), black carbon (BC), and organic carbon (OC) in India between 1995 and 2014 from the CEDS. Figure S5 indicates an overall increase in ANTHRO emissions before slowly falling after 2011. Significant inter-annual variations in BB emissions, such as in 1999, 2006, and 2009, were mainly caused by climate change-induced hot and arid conditions (Sahu et al., 2015). Figure S6 shows that ANTHRO emissions occurred predominately in IGP and central India, significantly increasing across all regions. Unlike other administrative regions, northern and eastern India, such as Punjab and Manipur, features a higher ratio of BB emissions to ANTHRO emissions.

3.2.2 The long-term trends of $PM_{2.5}$ and O_3 in India from 1995 to 2014

From the BASE simulation, we estimate that the annual mean pop-weighted $PM_{2.5}$ and O_3 for India in 1995 and 2014 were 29.88 μg m^{-3} and 67.41 ppbv, respectively. Figure 3a, b show that annual average $PM_{2.5}$ concentrations gradually rose from the south to the north, with high levels predominantly found in the IGP, mainly caused by high ANTHRO emissions (Fig. S6) and reduced ventilation due to obstruction by the Tibetan Plateau (Gao et al., 2018). Surface annual average O_3 concentrations gradually increased from west to east and south to north, with the highest levels concentrated in northern India and the eastern part of central India. The spatial patterns of the $PM_{2.5}$ and O_3 distribution in India are also seen in several previous studies, though they only discussed one or several specific years (Jia et al., 2021; Pandey et al., 2021).

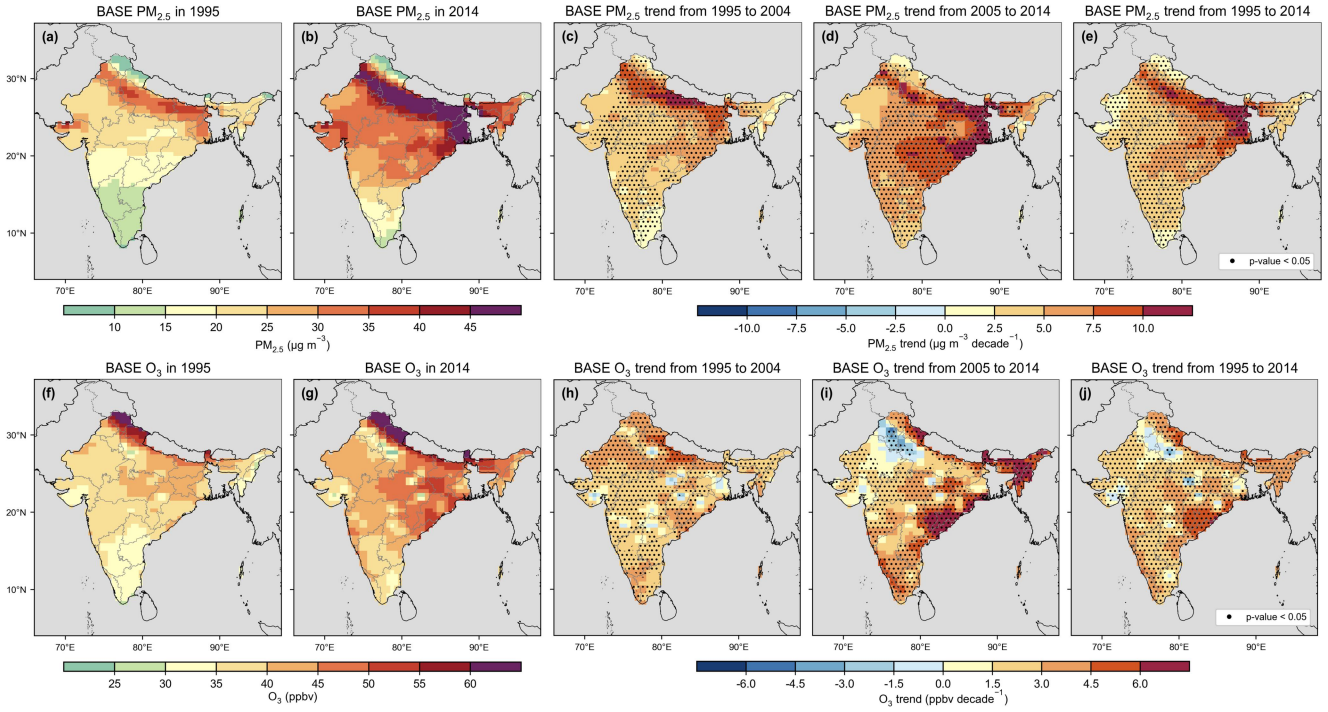

Figure 3. Spatial distributions of $PM_{2.5}$ (top panel) and O_3 (bottom panel) for annual average in 1995 (a, f) and 2014 (b, g), with the trends from 1995 to 2004 (c, h), 2005 to 2014 (d, i), and 1995 to 2014 (e, j). The black dot denotes the areas where the trend is statistically significant ($p < 0.05$). The units are μg m^{-3} for $PM_{2.5}$ (a,b) and ppbv for O_3 in (f, g), and μg m^{-3} per decade (μg m^{-3} $decade^{-1}$) for $PM_{2.5}$ trends (c,d,e), and ppbv per decade (ppbv $decade^{-1}$) for O_3 trends (h,i,j).

From Figure 3, we also find that both $PM_{2.5}$ and O_3 showed a statistically significant increasing trend all over the country from 1995 to 2014, with a nationwide increasing rate of 6.71 μg m^{-3} $decade^{-1}$ ($p < 0.01$) for pop-weighted $PM_{2.5}$ and 7.08 ppbv $decade^{-1}$ ($p < 0.01$) for pop-weighted O_3, respectively (Fig. S7), which was mainly driven by rapid industrialization and substantial economy development (Pandey et al., 2014; Sadavarte and Venkataraman, 2014). However, distinct spatial heterogeneity for the increasing trend was observed for the two air pollutants. $PM_{2.5}$ exhibited varying degrees of increase across India, with the most distinctive increase occurring in the IGP, where the maximum trend reached 12.60 μg m^{-3} $decade^{-1}$. This notable rise can be attributed to the increased regional ANTHRO emissions (Fig. S6). For O_3, eastern central India experienced the highest O_3 increases, with an obvious increase in the eastern and the lowest in western India. One thing needs to be pointed out that in northern IGP, including New Delhi, significant O_3 decreases were also observed, which could be caused by the inhibited O_3 production due to NO titration as a result of the dramatic increase in NOx emissions, as discussed in Karambelas et al. (2018). Splitting the trend into two periods (from 1995 to 2004 and from 2005 to 2014), we find a larger increasing trend in the latter period than that in the previous one for both $PM_{2.5}$ and O_3, which may be due to the rapid urbanization and growing transportation activities over populous regions (Fig. S8) in recent years in India (Gao et al., 2018).

3.3 Driving factor analysis for the air pollution changes in India

3.3.1 Contributions to the annual and seasonal trends

To disentangle the contributions of ANTHRO and BB emissions to long-term trends in $PM_{2.5}$ and O_3 concentrations in India from 1995 to 2014, we first analyze their contributions to annual and seasonal trends (Figure 4). Not surprisingly, changes in ANTHRO emissions dominated the deterioration of $PM_{2.5}$ and O_3 in India, consistent with studies based on observational and satellite data (Gurjar et al., 2016; Vohra et al., 2022). Changes in ANTHRO emissions alone increased area-weighted $PM_{2.5}$ by 5.46 μg m^{-3} $decade^{-1}$ ($p < 0.01$) and area-weighted O_3 by 2.71 ppbv $decade^{-1}$ ($p < 0.01$), accounting for 102.21% and 104.11% of the total changes, respectively. The contributions of changes in BB emissions were relatively minor, with distinct interannual variations and seasonal variations. Spatially, we found that both the long-term $PM_{2.5}$ and O_3 trends were mostly dominated by the ANTHRO emissions changes all over India (Fig. S9a, c). Changes in BB emissions led to a slightly increasing trend of $PM_{2.5}$ in most of India and a decreasing trend in eastern India, though neither was statistically significant. BB emissions seemed to increase O_3 in IGP and central India and decrease O_3 in western India, but the trends were insignificant (Fig. S9b, d).

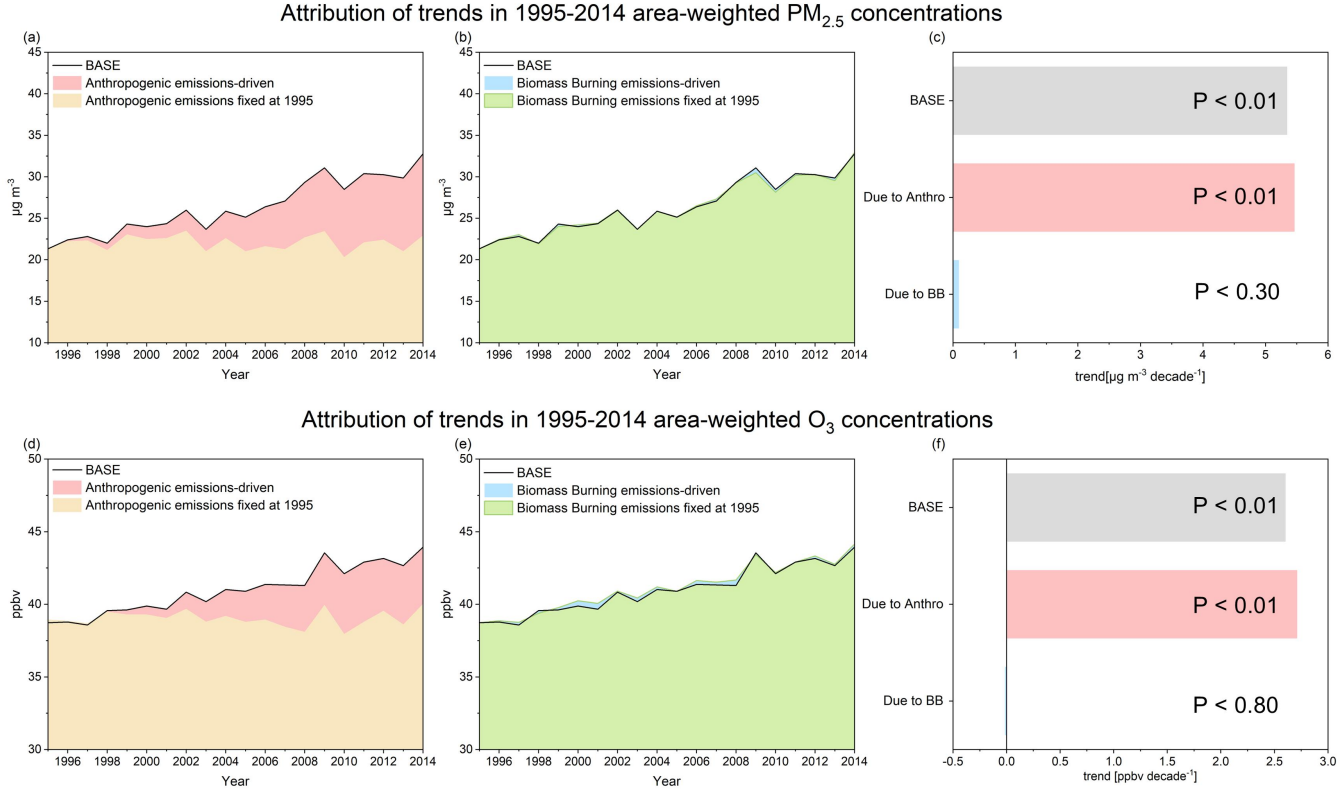

Figure 4. Drivers for trends of area-weighted (a-c) $PM_{2.5}$ and (d-f) O_3 in India in 1995-2014. The yellow shadings in (a, d) show the evolution of model-simulated $PM_{2.5}$ and O_3 concentrations in the FixAN simulation, with the red shadings illustrating the estimation of the $PM_{2.5}$ and O_3 concentrations resulting from changes in ANTHRO emissions compared to the 1995 level. (b, e) as

for (a, d), but for impacts of changes in BB emissions. (c, f) denotes the estimated $PM_{2.5}$ and O_3 trends in India derived from the BASE simulation and impacts of ANTHRO and BB emissions, respectively.

It is well recognized that BB emissions usually feature a distinct seasonal trend, especially in India, where monsoons influence them. Hence, here we quantify the seasonal trend of $PM_{2.5}$ and O_3 from ANTHRO and BB emissions for DJF (December-January-February), MAM (March-April-May), JJA (June-July-August, monsoon season), and SON (September-October-November, post-monsoon season) from 1995 to 2014 by subtracting the BASE scenario from the FixAN or FixBB scenarios. The annual trends for $PM_{2.5}$ and O_3 for each season were subsequently estimated using the Theil-Sen estimator and the Mann-Kendall test. From Fig. 5a-h, we find that the contributions of ANTHRO emissions had consistent spatial patterns for the seasonal $PM_{2.5}$ trend, with larger influences in the post-monsoon seasons (DJF and SON), which was estimated to be responsible for $PM_{2.5}$ enhancement by as high as 17.08 μg m^{-3} $decade^{-1}$ because of decreased vertical dispersion and diffusion of aerosol caused by lower solar radiation during winter and surface wind speeds (Bran and Srivastava, 2017). The contributions of ANTHRO emissions during the MAM and JJA were modulated as a result of increased precipitation, strong air convergence, and uplift strong air convergence during the presence of the summer monsoon, which impeded the accumulation of $PM_{2.5}$ concentrations at ground level (Bran and Srivastava, 2017; Gao et al., 2020; Lu et al., 2018). Unlike $PM_{2.5}$, the contributions of ANTHRO emissions changes on surface O_3 trend in India had a distinct spatial pattern across seasons (Fig. 5i-p). The ANTHRO emissions had a much stronger positive influence on the O_3 increases in northern, eastern central, and eastern India during JJA and SON, while it had the largest increases in southern India in the pre-monsoon season (MAM, Fig. 5j). It was reported that the stronger solar radiation and higher temperature in MAM were attributed to an increase in the photochemical efficiency of O_3 in the presence of NOx (Doherty et al., 2013; Jacob and Winner, 2009; Pusede et al., 2015). The decreased O_3 in the IGP was most pronounced in the DJF season (Fig. 5i), mainly attributed to lower solar radiation and titration of O_3 by higher NOx levels (Kumar et al., 2012). Additionally, the occurrence of winter monsoon led to extensive air subsidence in northern India, resulting in low net O_3 production and strong horizontal export, ultimately leading to relatively low O_3 levels (Lu et al., 2018).

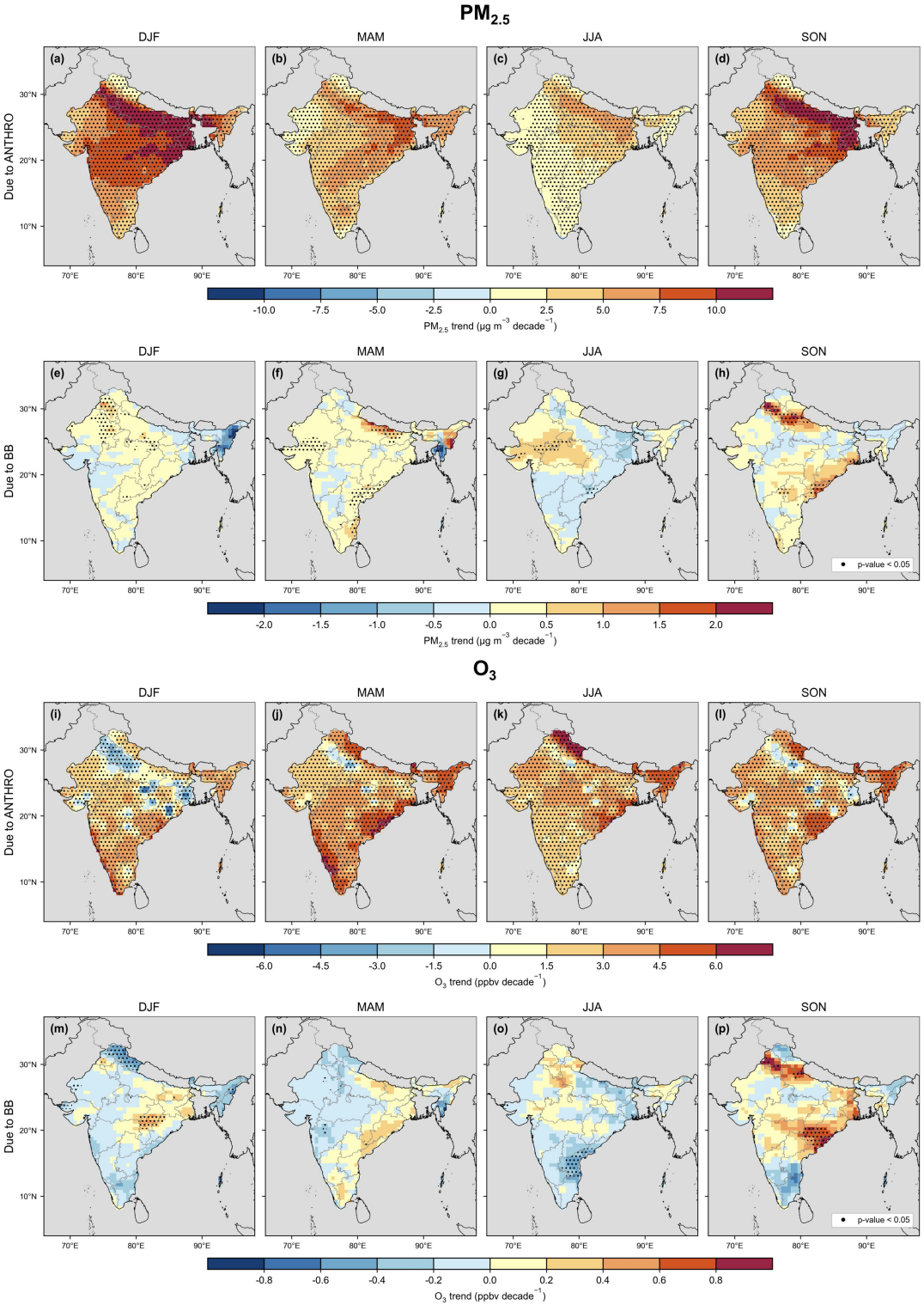
PM2.5
DJF
MAM
JJA
SON
(a)
(b)
(c)
(d)
Due to ANTHRO
30°N
20°N
10°N
70°E
80°E
90°E
-10.0
-7.5
-5.0
-2.5
0.0
2.5
5.0
7.5
10.0
PM2.5 trend (μg m−3 decade−1)
(e)
(f)
(g)
(h)
Due to BB
p-value < 0.05
-2.0
-1.5
-1.0
-0.5
0.0
0.5
1.0
1.5
2.0
PM2.5 trend (μg m−3 decade−1)
O3
(i)
(j)
(k)
(l)
-6.0
-4.5
-3.0
-1.5
0.0
1.5
3.0
4.5
6.0
O3 trend (ppbv decade−1)
(m)
(n)
(o)
(p)
-0.8
-0.6
-0.4
-0.2
0.0
0.2
0.4
0.6
0.8
O3 trend (ppbv decade−1)

Figure 5. Seasonal patterns of (a-d) ANTHRO and (e-h) BB emissions contributions for the trends of $PM_{2.5}$ in India from 1995 to 2014 and (i-p) for O_3. The units are μg m^{-3} per decade for $PM_{2.5}$ and ppbv per decade for O_3. The dots in the plots indicate statistically significant trends, with p-values less than 0.05.

3.3.2 Contributions to the seasonal air quality changes

BB emissions exhibit a high degree of interannual variability, leading to less clear trends in the annual data. Thus, Figure 6 focuses on the spatial distributions of BB contributions for seasonal $PM_{2.5}$ and O_3 changes between 1995 and 2014 rather than trends, as detailed in Table S4. These contributions are quantified by subtracting the BASE scenario in 2014 from the FixBB scenario in 2014. The changes in BB emissions from 1995 to 2014 contributed significantly to the $PM_{2.5}$ increases in eastern India (over 20 μg m^{-3}) with a high incidence of forest fires (Jena et al., 2015). It also led to an increase of O_3 by more than 4 ppbv in eastern India in MAM. Contributions to seasonal $PM_{2.5}$ and O_3 changes from BB were comparable to or even exceeded those from ANTHRO in some regions, such as Manipur and Nagaland (Fig. S10). With a higher BB fraction in other years, such as 1999, these contributions could even be even higher, reaching up to 46.03 μg m^{-3} and 6.46 ppbv for $PM_{2.5}$ and O_3, respectively (Fig. S11). Therefore, despite their variability, the BB emissions in India posed a great threat to the air quality and thus could not be overlooked.

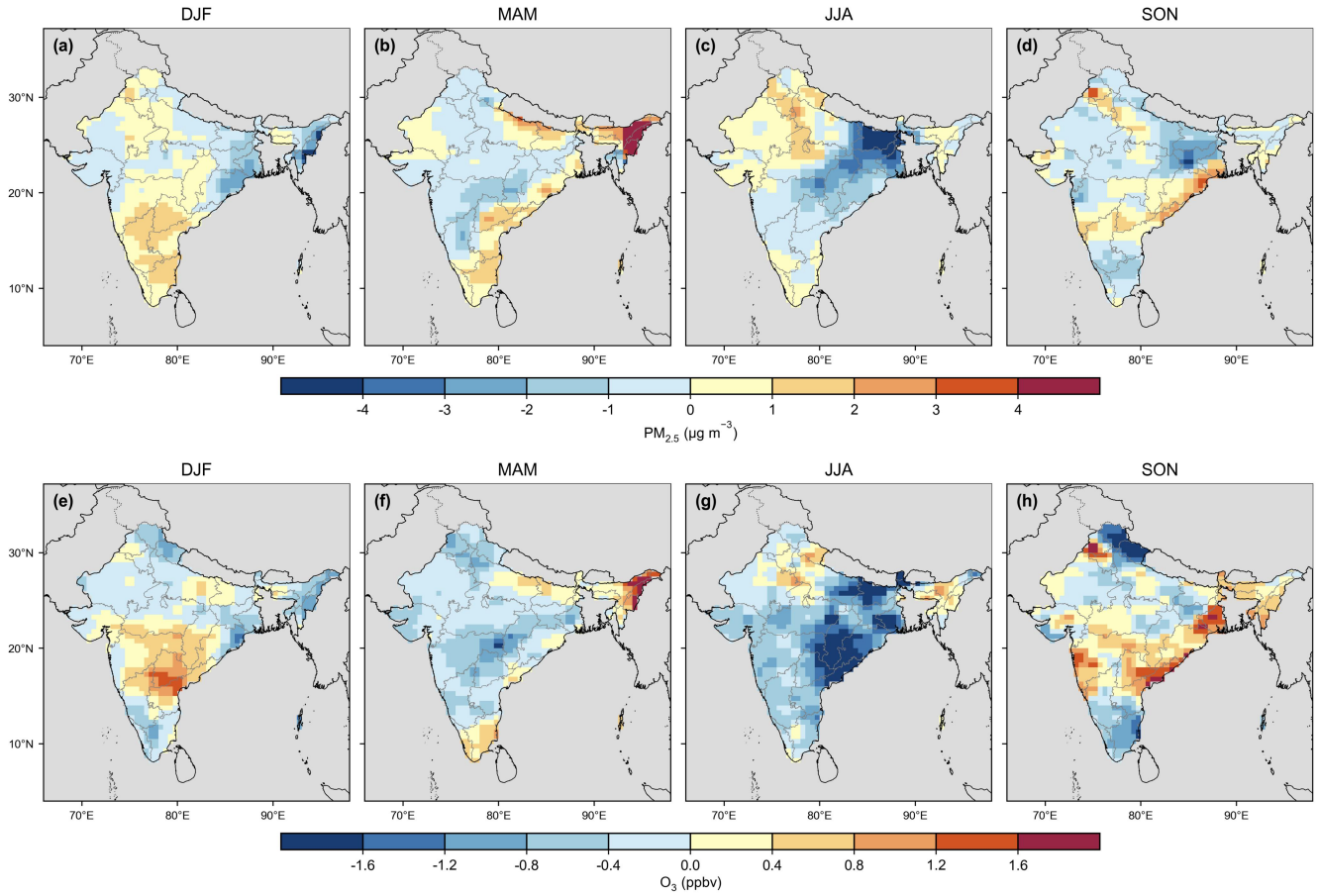

Figure 6. Spatial distributions of the BB contribution for seasonal (a-d) $PM_{2.5}$ and (e-h) O_3 changes from 1995 to 2014 for DJF, MAM, JJA, and SON. The contributions from BB were calculated as the differences between BASE and FixBB in 2014. The units are μg m^{-3} and ppbv.

3.4 Long-term trends of premature mortality due to $PM_{2.5}$ and O_3 in India

We estimate that the national mortality burden attributable to ambient $PM_{2.5}$ exposure rose significantly from 698.29 thousand in 1995 to 893.33 thousand in 2014, at a rate of 97.83 thousand per decade ($p < 0.01$, Figure 7a). Similarly, the mortality burden attributable to O_3 exposure also notably rose from 414.50 thousand in 1995 to 580.03 thousand in 2014, 73.91 thousand per decade ($p < 0.01$). The hotspots of premature mortality attributable to $PM_{2.5}$ and O_3 exposure occurred in New Delhi and IGP regions in 1995 and 2014 (Fig. 7b-e), coincidently with the dense population (Fig. S8). We find that Uttar Pradesh, Bihar, West Bengal, and Haryana, four states within the IGP region, accounted for 41.00% and 39.77% of the national premature mortality due to $PM_{2.5}$ and O_3 in 2014, respectively. Considering this heterogeneous spatial distribution, it is imperative for the IGP region to implement stronger air pollution control policies to safeguard human health, as discussed by Jia et al. (2021). Our estimations for the O_3-related mortality burden are higher than those reported from the GBD2019 (Fig. S12) since we applied a higher RR and used larger baseline mortality rates (see Methods section 2.4). After

recalculating the O_3-related mortality burden using the GBD2019 metrics, we report an increasing trend of 29.74 thousand deaths per decade^{-1} for O_3-related mortality, comparable to the GBD2019 estimation of 33.24 thousand deaths per decade^{-1}. However, our estimated mortality burdens are still slightly higher than the GBD2019 due to the O_3 overestimation in our model (Fig. 2 and Fig. S4).

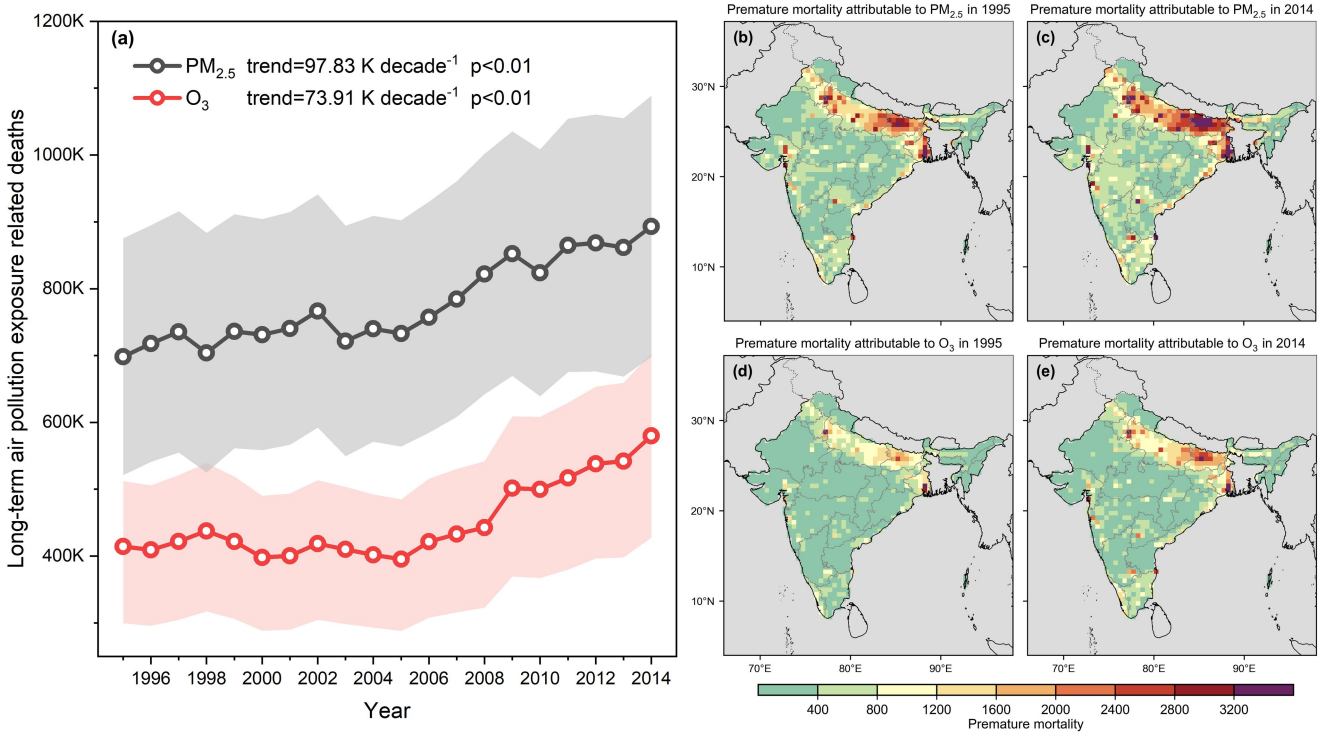

Figure 7. Spatial-temporal change of mortality burden attributable to $PM_{2.5}$ and O_3. (a) interannual variation from 1995 to 2014. The shaded area indicates the range of 95% confidence interval account for RR estimates of long-term exposure to $PM_{2.5}$ and O_3 (gray indicates half of the range). (b-e) spatial distributions of the average annual premature mortality attributable to (b-c) $PM_{2.5}$ and (d-e) O_3 in 1995 and 2014.

To isolate the effects of population heterogeneous among regions, we also quantify the mortality burden changes per capita (avoided deaths per 100,000 people) from 1995 to 2014 (Fig. 8). $PM_{2.5}$-attributable premature mortality per capita was higher in the IGP and eastern India, with the highest in Chandigarh (427.2), followed by Sikkim (153.6), Meghalaya (140.3), and NCT of Delhi (126.1) in 1995 (Fig. S13). The spatial distribution of O_3-attributable premature mortality per capita resembled that of $PM_{2.5}$. However, the values were relatively smaller, with the maximum value also appearing in Chandigarh (288.0), followed by Sikkim (120.2), Meghalaya (68.6), and NCT of Delhi (68.0) in 1995 (Fig. S13). Over the period from 1995 to 2014, $PM_{2.5}$- and O_3- attributable premature mortality per capita decreased in the north and increased in the south (Fig. 8), indicating that the increasing trend of premature mortality attributable to $PM_{2.5}$ and O_3 in the IGP region was mainly driven by the increased population (Fig. S8).

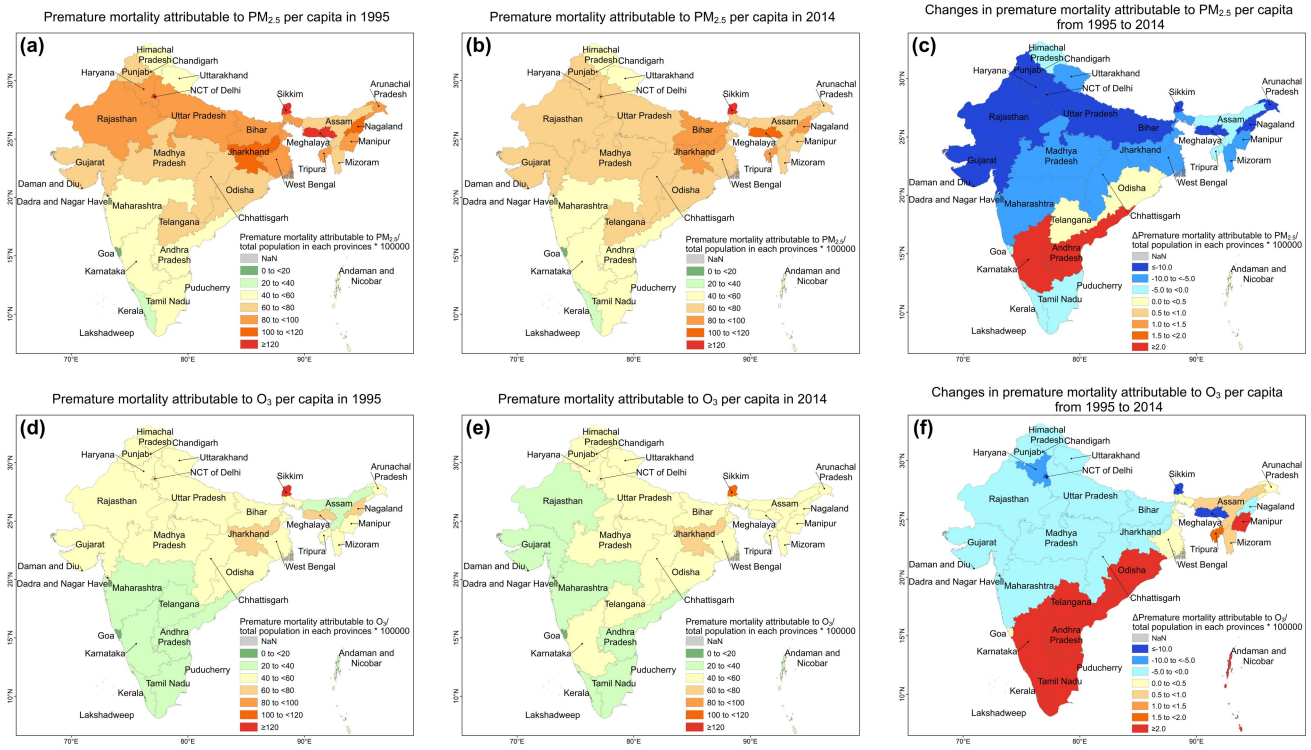

Figure 8. Spatial distributions of premature mortality attributable to $PM_{2.5}$ or O_3 per capita (avoid deaths per 100,000 people) in (a, d) 1995, (b, e) 2014, and (c, f) changes from 1995 to 2014 in the state of India.

Figure 9 shows that changes in ANTHRO emissions from 1995 to 2014 increased premature mortality per capita attributable to $PM_{2.5}$, with the higher values located mainly in eastern IGP and central India. Changes in BB emissions increased premature mortality attributable to $PM_{2.5}$ per capita in eastern, western, and southern India and decreased in IGP and central India. The state with the largest increase was Manipur (2.55), followed by Nagaland (2.06), associated with the high incidence of wildfires in these regions. The state that experienced the largest decrease was Jharkhand (-1.71), with Bihar (-1.02) followed behind. To explore contribution changes from ANTHRO and BB emissions, we estimate the premature mortality attributable to $PM_{2.5}$ per capita in 2000, 2005, and 2010-2014 in Table S5, respectively, consistent with the demonstrations from GBD2017. There was a sharp rise in contributions to premature mortality attributable to $PM_{2.5}$ from changes in ANTHRO emissions from 1995 to 2014. Not surprisingly, the premature mortality attributable to $PM_{2.5}$ from changes in BB emissions fluctuated greatly from 1995 to 2014. In 2000, a year with high BB emissions (Fig. S5), the contributions of changes in BB emissions to the premature mortality attributable to $PM_{2.5}$ in the states of Mizoram, Nagaland, Arunachal Pradesh, and Tripura reached 5.14, 4.90, 4.86, and 4.17, respectively, which exceeding the contributions of changes in ANTHRO emissions in that year (Table S5).

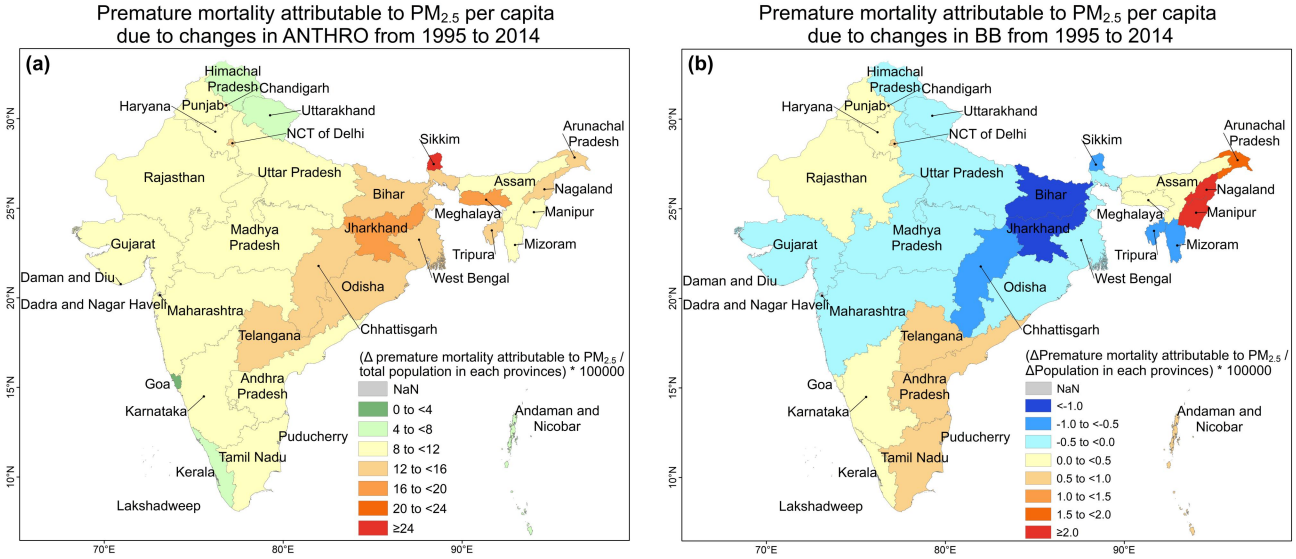

Figure 9. Spatial distributions of contributions to premature mortality attributable to $PM_{2.5}$ per capita (avoided deaths per 100,000 people) from changes in (a) ANTHRO and (b) BB emissions from 1995 to 2014.

4 Conclusions

In this study, we apply a state-of-the-art global CTM (CAM-chem) to provide a detailed assessment of long-term trends of the ambient annual mean $PM_{2.5}$ and O_3 in India and their health burden from 1995 to 2014, as well as the driving factor from ANTHRO and BB emissions changes. The annual mean area-weighted $PM_{2.5}$ over India increased at 5.34 μg m^{-3} $decade^{-1}$ ($p < 0.01$) from 1995 to 2014, dominated by the ANTHRO emissions (5.46 μg m^{-3} $decade^{-1}$, $p < 0.01$). The highest and fastest $PM_{2.5}$ growth was in the IGP regions due to the rapid industrialization, urbanization, and transportation growth. For annual mean area-weighted O_3, the increase was 2.60 ppbv $decade^{-1}$ ($p < 0.01$), dominated by the ANTHRO emissions as well (2.71 ppbv $decade^{-1}$, $p < 0.01$). We find that O_3 concentrations were highest in northern India, with the fastest growth occurring in northern, central, and eastern India. The contributions from BB emissions for the long-term trends were not significant for either $PM_{2.5}$ (0.09 μg m^{-3} $decade^{-1}$, $p < 0.30$) or O_3 (-0.01, $p < 0.80$) and showed significant seasonal variations due to large inter-annual variability features. However, when we examine the air quality changes in specific years, such as 1999 and 2014, when there were larger BB activities in India, we found that the contributions from BB could be comparable to or even exceed those from ANTHRO during DJF and MAM, reaching over 46.03 μg m^{-3} and 6.46 ppbv for $PM_{2.5}$ and O_3, respectively.

Further estimation of mortality burden shows a 27.93% (698.29 to 893.33 thousand) increase in premature mortality attributable to $PM_{2.5}$ between 1995 and 2014 (22.94% for 2005-2014), and a 39.93% (414.50 to 580.03 thousand) increase for O_3 (44.54% increasing during 2005-2014). Changes in ANTHRO and BB emissions were responsible for an

enhancement of premature mortality attributable to $PM_{2.5}$ by 88.78% (97.83 thousand per decade, $p < 0.01$) and 0.02% (2.38 thousand per decade, $p < 0.10$). After removing the effect of population growth, our analysis reveals a notably higher mortality burden per capita attributable to $PM_{2.5}$ in the IGP regions. However, it was noteworthy that the mortality burden per capita in these regions exhibited a significant decline over the period of 1995-2014, despite the increasing trend of premature mortality. This suggests that population growth was the primary factor driving the trend of premature mortality.

Our study is subject to several uncertainties and limitations. First of all, the coarser resolution in the global model (0.9° × 1.25°) frequently cannot realistically represent the complex physical and chemical processes of regional-scale air pollution, especially for O_3 (Yue et al., 2023). Moreover, missing chemical mechanisms in the model, such as the lack of representations of nitrate and ammonium (Ren et al., 2023) and the secondary organic aerosol (Liu et al., 2021), prevented the model from accurately simulating $PM_{2.5}$ concentration, especially during heavily polluted regions, such as China and India (Turnock et al., 2020). Another major uncertainty originated from the inaccurate emission inventory, especially for developing regions in early periods, as reported by the global datasets (Paulot et al., 2018; Wang et al., 2022). Zhang et al. (2021b) revealed that model performance with global CEDS inventory tends to predict lower bias for surface $PM_{2.5}$ and higher bias for surface O_3 compared with a regional emission inventory (MEIC) in China due to disparities in spatial allocation. Xie et al. (2024) also highlighted a significant underestimation of agricultural fires in the inventory. Moreover, the uncertainty from health functions ranging from the choice of the exposure-response functions (Ostro et al., 2018; Giani et al., 2020) and the uncertainties of the baseline mortality rates both had different impacts on human health (Lelieveld et al., 2015; Pozzer et al., 2023). Meanwhile, in estimating the mortality burden, we apply the RR derived from a global study rather than using values specific to India, which could potentially be lower (Brown et al., 2022). Thus, our estimations for the air pollution-related mortality burden could be overestimated. More epidemiology studies should be conducted in India to retrieve their RR. Finally, another limitation in our experimental design was that we set global fixed emissions for ANTHRO and BB instead of in India only, ignoring the impact of intercontinental transportation.

Code and data availability

The CESM model code is available at https://www.cesm.ucar.edu/models/cesm2/release_download.html (last access: 12 March 2024). Observation data is available at https://wustl.box.com/s/79pfex658crbq4dykxh51vvfdpksfhj5 (last access: 29 March 2024), which is collected by the Atmospheric Composition Analysis Group (ACAG) at Washington University in St. Louis.

Author contributing

B.L. analyzed the simulation results and wrote the manuscript. Y.Z. and T.T. conceived the idea, designed and conducted the experiment. Y.Z., T.T., H.Z., J.H., J.M., W.W., and L.X. revised the original paper. All authors contributed to the manuscript.

Competing interests

The authors declare that they have no conflict of interest.

Acknowledgments

This work was supported by the National Natural Science Foundation of China (42375172). We would like to acknowledge the Atmospheric Composition Analysis Group, the Washington University in St. Louis (WUSTL), for providing open access to the satellite-derived $PM_{2.5}$ (https://sites.wustl.edu/acag/datasets/surface-pm2-5/, last accessed on March 18, 2024). We also acknowledge the High Performance Computer resources (2023-EL-PT-000184) from the National Key Scientific and Technological Infrastructure project "Earth System Numerical Simulation Facility" (EarthLab). This material is based upon work supported by the National Center for Atmospheric Research, which is a major facility sponsored by the NSF under cooperative agreement no. 1852977. We thank all the scientists, software engineers, and administrators who contributed to the development of CESM2.

References

Agarwal, P., Stevenson, D. S., and Heal, M. R.: Evaluation of WRF-Chem-simulated meteorology and aerosols over northern India during the severe pollution episode of 2016, Atmospheric Chemistry and Physics, 24, 2239–2266, https://doi.org/10.5194/acp-24-2239-2024, 2024.

Bran, S. H. and Srivastava, R.: Investigation of $PM_{2.5}$ mass concentration over India using a regional climate model, Environmental Pollution, 224, 484–493, https://doi.org/10.1016/j.envpol.2017.02.030, 2017.

Brown, P. E., Izawa, Y., Balakrishnan, K., Fu, S. H., Chakma, J., Menon, G., Dikshit, R., Dhaliwal, R. S., Rodriguez, P. S., Huang, G., Begum, R., Hu, H., D'Souza, G., Guleria, R., and Jha, P.: Mortality Associated with Ambient $PM_{2.5}$ Exposure in India: Results from the Million Death Study, Environmental Health Perspectives, 130, 097004, https://doi.org/10.1289/EHP9538, 2022.

Burnett, R. T., Pope, C. A., Ezzati, M., Olives, C., Lim, S. S., Mehta, S., Shin, H. H., Singh, G., Hubbell, B., Brauer, M., Anderson, H. R., Smith, K. R., Balmes, J. R., Bruce, N. G., Kan, H., Laden, F., Pr, üss-U. A., Turner, M. C., Gapstur, S. M., Diver, W. R., and Cohen, A.: An Integrated Risk Function for Estimating the Global Burden of Disease Attributable to Ambient Fine Particulate Matter Exposure, Environmental Health Perspectives, 122, 397–403, https://doi.org/10.1289/ehp.1307049, 2014.

Carvalho, A., Monteiro, A., Flannigan, M., Solman, S., Miranda, A. I., and Borrego, C.: Forest fires in a changing climate and their impacts on air quality, Atmospheric Environment, 45, 5545–5553, https://doi.org/10.1016/j.atmosenv.2011.05.010, 2011.

Christiansen, A. E., Carlton, A. G., and Porter, W. C.: Changing Nature of Organic Carbon over the United States, Environ. Sci. Technol., 54, 10524–10532, https://doi.org/10.1021/acs.est.0c02225, 2020.

Conibear, L., Butt, E. W., Knote, C., Spracklen, D. V., and Arnold, S. R.: Current and Future Disease Burden From Ambient Ozone Exposure in India, GeoHealth, 2, 334–355, https://doi.org/10.1029/2018GH000168, 2018a.

Conibear, L., Butt, E. W., Knote, C., Arnold, S. R., and Spracklen, D. V.: Residential energy use emissions dominate health impacts from exposure to ambient particulate matter in India, Nat Commun, 9, 617, https://doi.org/10.1038/s41467-018-02986-7, 2018b.

Crutzen, P. J. and Andreae, M. O.: Biomass Burning in the Tropics: Impact on Atmospheric Chemistry and Biogeochemical Cycles, Science, 250, 1669–1678, https://doi.org/10.1126/science.250.4988.1669, 1990.

Danabasoglu, G., Lamarque, J.-F., Bacmeister, J., Bailey, D. A., DuVivier, A. K., Edwards, J., Emmons, L. K., Fasullo, J., Garcia, R., Gettelman, A., Hannay, C., Holland, M. M., Large, W. G., Lauritzen, P. H., Lawrence, D. M., Lenaerts, J. T. M., Lindsay, K., Lipscomb, W. H., Mills, M. J., Neale, R., Oleson, K. W., Otto-Bliesner, B., Phillips, A. S., Sacks, W., Tilmes, S., van Kampenhout, L., Vertenstein, M., Bertini, A., Dennis, J., Deser, C., Fischer, C., Fox-Kemper, B., Kay, J. E., Kinnison, D., Kushner, P. J., Larson, V. E., Long, M. C., Mickelson, S., Moore, J. K., Nienhouse, E., Polvani, L., Rasch, P. J., and Strand, W. G.: The Community Earth System Model Version 2 (CESM2), Journal of Advances in Modeling Earth Systems, 12, e2019MS001916, https://doi.org/10.1029/2019MS001916, 2020.

David, L. M., Ravishankara, A. R., Kodros, J. K., Venkataraman, C., Sadavarte, P., Pierce, J. R., Chaliyakunnel, S., and Millet, D. B.: Aerosol Optical Depth Over India, Journal of Geophysical Research: Atmospheres, 123, 3688–3703, https://doi.org/10.1002/2017JD027719, 2018.

Dedoussi, I. C., Eastham, S. D., Monier, E., and Barrett, S. R. H.: Premature mortality related to United States cross-state air pollution, Nature, 578, 261–265, https://doi.org/10.1038/s41586-020-1983-8, 2020.

Doherty, R. M., Wild, O., Shindell, D. T., Zeng, G., MacKenzie, I. A., Collins, W. J., Fiore, A. M., Stevenson, D. S., Dentener, F. J., Schultz, M. G., Hess, P., Derwent, R. G., and Keating, T. J.: Impacts of climate change on surface ozone and intercontinental ozone pollution: A multi-model study, Journal of Geophysical Research: Atmospheres, 118, 3744–3763, https://doi.org/10.1002/jgrd.50266, 2013.

van Donkelaar, A., Hammer, M. S., Bindle, L., Brauer, M., Brook, J. R., Garay, M. J., Hsu, N. C., Kalashnikova, O. V., Kahn, R. A., Lee, C., Levy, R. C., Lyapustin, A., Sayer, A. M., and Martin, R. V.: Monthly Global Estimates of Fine Particulate Matter and Their Uncertainty, Environ. Sci. Technol., 55, 15287–15300, https://doi.org/10.1021/acs.est.1c05309, 2021.

Emmons, L. K., Schwantes, R. H., Orlando, J. J., Tyndall, G., Kinnison, D., Lamarque, J.-F., Marsh, D., Mills, M. J., Tilmes, S., Bardeen, C., Buchholz, R. R., Conley, A., Gettelman, A., Garcia, R., Simpson, I., Blake, D. R., Meinardi, S., and Pétron, G.: The Chemistry Mechanism in the Community Earth System Model Version 2 (CESM2), Journal of Advances in Modeling Earth Systems, 12, e2019MS001882, https://doi.org/10.1029/2019MS001882, 2020.

Fuller, R., Landrigan, P. J., Balakrishnan, K., Bathan, G., Bose-O'Reilly, S., Brauer, M., Caravanos, J., Chiles, T., Cohen, A., Corra, L., Cropper, M., Ferraro, G., Hanna, J., Hanrahan, D., Hu, H., Hunter, D., Janata, G., Kupka, R., Lanphear, B., Lichtveld, M., Martin, K., Mustapha, A., Sanchez-Triana, E., Sandilya, K., Schaefli, L., Shaw, J., Seddon, J., Suk, W., Téllez-Rojo, M. M., and Yan, C.: Pollution and health: a progress update, The Lancet Planetary Health, 6, e535–e547, https://doi.org/10.1016/S2542-5196(22)00090-0, 2022.

Gao, M., Beig, G., Song, S., Zhang, H., Hu, J., Ying, Q., Liang, F., Liu, Y., Wang, H., Lu, X., Zhu, T., Carmichael, G. R., Nielsen, C. P., and McElroy, M. B.: The impact of power generation emissions on ambient $PM_{2.5}$ pollution and human health in China and India, Environment International, 121, 250–259, https://doi.org/10.1016/j.envint.2018.09.015, 2018.

Gao, M., Gao, J., Zhu, B., Kumar, R., Lu, X., Song, S., Zhang, Y., Jia, B., Wang, P., Beig, G., Hu, J., Ying, Q., Zhang, H., Sherman, P., and McElroy, M. B.: Ozone pollution over China and India: seasonality and sources, Atmospheric Chemistry and Physics, 20, 4399–4414, https://doi.org/10.5194/acp-20-4399-2020, 2020.

GBD 2015 Risk Factors Collaborators: Global, regional, and national comparative risk assessment of 79 behavioural, environmental and occupational, and metabolic risks or clusters of risks, 1990–2015: a systematic analysis for the Global Burden of Disease Study 2015, The Lancet, 388, 1659–1724, https://doi.org/10.1016/S0140-6736(16)31679-8, 2016.

GBD 2017 Risk Factor Collaborators: Global, regional, and national comparative risk assessment of 84 behavioural, environmental and occupational, and metabolic risks or clusters of risks for 195 countries and territories, 1990–2017: a systematic analysis for the Global Burden of Disease Study 2017, The Lancet, 392, 1923–1994, https://doi.org/10.1016/S0140-6736(18)32225-6, 2018.

GBD 2019 Risk Factors Collaborators: Global burden of 87 risk factors in 204 countries and territories, 1990–2019: a systematic analysis for the Global Burden of Disease Study 2019, The Lancet, 396, 1223–1249, https://doi.org/10.1016/S0140-6736(20)30752-2, 2020.

Giani, P., Castruccio, S., Anav, A., Howard, D., Hu, W., and Crippa, P.: Short-term and long-term health impacts of air pollution reductions from COVID-19 lockdowns in China and Europe: a modelling study, The Lancet Planetary Health, 4, e474–e482, https://doi.org/10.1016/S2542-5196(20)30224-2, 2020.

Gurjar, B. R., Ravindra, K., and Nagpure, A. S.: Air pollution trends over Indian megacities and their local-to-global implications, Atmospheric Environment, 142, 475–495, https://doi.org/10.1016/j.atmosenv.2016.06.030, 2016.

Guttikunda, S. and Ka, N.: Evolution of India's $PM_{2.5}$ pollution between 1998 and 2020 using global reanalysis fields coupled with satellite observations and fuel consumption patterns, Environ. Sci.: Atmos., 2, 1502–1515, https://doi.org/10.1039/D2EA00027J, 2022.

Hoek, G., Krishnan, R. M., Beelen, R., Peters, A., Ostro, B., Brunekreef, B., and Kaufman, J. D.: Long-term air pollution exposure and cardio- respiratory mortality: a review, Environ Health, 12, 43, https://doi.org/10.1186/1476-069X-12-43, 2013.

Hoesly, R. M., Smith, S. J., Feng, L., Klimont, Z., Janssens-Maenhout, G., Pitkanen, T., Seibert, J. J., Vu, L., Andres, R. J., Bolt, R. M., Bond, T. C., Dawidowski, L., Kholod, N., Kurokawa, J., Li, M., Liu, L., Lu, Z., Moura, M. C. P., O'Rourke, P. R., and Zhang, Q.: Historical (1750–2014) anthropogenic emissions of reactive gases and aerosols from the Community Emissions Data System (CEDS), Geoscientific Model Development, 11, 369–408, https://doi.org/10.5194/gmd-11-369-2018, 2018.

Hou, X., Wild, O., Zhu, B., and Lee, J.: Future tropospheric ozone budget and distribution over east Asia under a net-zero scenario, Atmospheric Chemistry and Physics, 23, 15395–15411, https://doi.org/10.5194/acp-23-15395-2023, 2023.

Huang, T., Ma, J., Song, S., Ling, Z., Macdonald, R. W., Gao, H., Tao, S., Shen, H., Zhao, Y., Liu, X., Tian, C., Li, Y., Jia, H., Lian, L., and Mao, X.: Health and environmental consequences of crop residue burning correlated with increasing crop yields midst India's Green Revolution, npj Clim Atmos Sci, 5, 1–9, https://doi.org/10.1038/s41612-022-00306-x, 2022.

Hystad, P., Demers, P. A., Johnson, K. C., Carpiano, R. M., and Brauer, M.: Long-term Residential Exposure to Air Pollution and Lung Cancer Risk, Epidemiology, 24, 762, https://doi.org/10.1097/EDE.0b013e3182949ae7, 2013.

India State-Level Disease Burden Initiative Air Pollution Collaborators: Health and economic impact of air pollution in the states of India: the Global Burden of Disease Study 2019, The Lancet Planetary Health, 5, e25–e38, https://doi.org/10.1016/S2542-5196(20)30298-9, 2021.

Jacob, D. J. and Winner, D. A.: Effect of climate change on air quality, Atmospheric Environment, 43, 51–63, https://doi.org/10.1016/j.atmosenv.2008.09.051, 2009.

Jain, M., Saxena, P., Sharma, S., and Sonwani, S.: Investigation of Forest Fire Activity Changes Over the Central India Domain Using Satellite Observations During 2001–2020, GeoHealth, 5, e2021GH000528, https://doi.org/10.1029/2021GH000528, 2021.

Jena, C., Ghude, S. D., Pfister, G. G., Chate, D. M., Kumar, R., Beig, G., Surendran, D. E., Fadnavis, S., and Lal, D. M.: Influence of springtime biomass burning in South Asia on regional ozone (O_3): A model based case study, Atmospheric Environment, 100, 37–47, https://doi.org/10.1016/j.atmosenv.2014.10.027, 2015.

Jia, B., Gao, M., Zhang, X., Xiao, X., Zhang, S., and Lam Yung, K. K.: Rapid increase in mortality attributable to $PM_{2.5}$ exposure in India over 1998–2015, Chemosphere, 269, 128715, https://doi.org/10.1016/j.chemosphere.2020.128715, 2021.

Karambelas, A., Holloway, T., Kinney, P. L., Fiore, A. M., DeFries, R., Kiesewetter, G., and Heyes, C.: Urban versus rural health impacts attributable to $PM_{2.5}$ and O_3 in northern India, Environ. Res. Lett., 13, 064010, https://doi.org/10.1088/1748-9326/aac24d, 2018.

Kumar, R., Naja, M., Pfister, G. G., Barth, M. C., Wiedinmyer, C., and Brasseur, G. P.: Simulations over South Asia using the Weather Research and Forecasting model with Chemistry (WRF-Chem): chemistry evaluation and initial results, Geoscientific Model Development, 5, 619–648, https://doi.org/10.5194/gmd-5-619-2012, 2012.

Lan, R., Eastham, S. D., Liu, T., Norford, L. K., and Barrett, S. R. H.: Air quality impacts of crop residue burning in India and mitigation alternatives, Nat Commun, 13, 6537, https://doi.org/10.1038/s41467-022-34093-z, 2022.

Latha, K. M. and Badarinath, K.: Seasonal variations of PM $_{10}$ and PM $_{2.5}$ particles loading over tropical urban environment, International Journal of Environmental Health Research, 15, 63–68, https://doi.org/10.1080/09603120400018964, 2005.

Lelieveld, J., Evans, J. S., Fnais, M., Giannadaki, D., and Pozzer, A.: The contribution of outdoor air pollution sources to premature mortality on a global scale, Nature, 525, 367–371, https://doi.org/10.1038/nature15371, 2015.

Liu, Y., Dong, X., Wang, M., Emmons, L. K., Liu, Y., Liang, Y., Li, X., and Shrivastava, M.: Analysis of secondary organic aerosol simulation bias in the Community Earth System Model (CESM2.1), Atmospheric Chemistry and Physics, 21, 8003–8021, https://doi.org/10.5194/acp-21-8003-2021, 2021.

Lu, X., Zhang, L., Liu, X., Gao, M., Zhao, Y., and Shao, J.: Lower tropospheric ozone over India and its linkage to the South Asian monsoon, Atmospheric Chemistry and Physics, 18, 3101–3118, https://doi.org/10.5194/acp-18-3101-2018, 2018.

van Marle, M. J. E., Kloster, S., Magi, B. I., Marlon, J. R., Daniau, A.-L., Field, R. D., Arneth, A., Forrest, M., Hantson, S., Kehrwald, N. M., Knorr, W., Lasslop, G., Li, F., Mangeon, S., Yue, C., Kaiser, J. W., and van der Werf, G. R.: Historic global biomass burning emissions for CMIP6 (BB4CMIP) based on merging satellite observations with proxies and fire models (1750–2015), Geoscientific Model Development, 10, 3329–3357, https://doi.org/10.5194/gmd-10-3329-2017, 2017.

McDuffie, E. E., Smith, S. J., O'Rourke, P., Tibrewal, K., Venkataraman, C., Marais, E. A., Zheng, B., Crippa, M., Brauer, M., and Martin, R. V.: A global anthropogenic emission inventory of atmospheric pollutants from sector- and fuel-specific sources (1970–2017): an application of the Community Emissions Data System (CEDS), Earth System Science Data, 12, 3413–3442, https://doi.org/10.5194/essd-12-3413-2020, 2020.

Miranda, A. I., Ferreira, J., Valente, J., Santos, P., Amorim, J. H., and Borrego, C.: Smoke measurements during Gestosa-2002 experimental field fires, Int. J. Wildland Fire, 14, 107, https://doi.org/10.1071/WF04069, 2005.

Munir, S., Habeebullah, T. M., Seroji, A. R., Gabr, S. S., Mohammed, A. M. F., and Morsy, E. A.: Quantifying temporal trends of atmospheric pollutants in Makkah (1997–2012), Atmospheric Environment, 77, 647–655, https://doi.org/10.1016/j.atmosenv.2013.05.075, 2013.

Ostro, B., Spadaro, J. V., Gumy, S., Mudu, P., Awe, Y., Forastiere, F., and Peters, A.: Assessing the recent estimates of the global burden of disease for ambient air pollution: Methodological changes and implications for low- and middle-income countries, Environmental Research, 166, 713–725, https://doi.org/10.1016/j.envres.2018.03.001, 2018.

Pandey, A., Sadavarte, P., Rao, A. B., and Venkataraman, C.: Trends in multi-pollutant emissions from a technology-linked inventory for India: II. Residential, agricultural and informal industry sectors, Atmospheric Environment, 99, 341–352, https://doi.org/10.1016/j.atmosenv.2014.09.080, 2014.

Panwar, T. S., Hooda, R. K., Lihavainen, H., Hyvarinen, A. P., Sharma, V. P., and Viisanen, Y.: Atmospheric aerosols at a regional background Himalayan site—Mukteshwar, India, Environ Monit Assess, 185, 4753–4764, https://doi.org/10.1007/s10661-012-2902-8, 2013.

Paulot, F., Paynter, D., Ginoux, P., Naik, V., and Horowitz, L. W.: Changes in the aerosol direct radiative forcing from 2001 to 2015: observational constraints and regional mechanisms, Atmospheric Chemistry and Physics, 18, 13265–13281, https://doi.org/10.5194/acp-18-13265-2018, 2018.

Pozzer, A., Anenberg, S. C., Dey, S., Haines, A., Lelieveld, J., and Chowdhury, S.: Mortality Attributable to Ambient Air Pollution: A Review of Global Estimates, GeoHealth, 7, e2022GH000711, https://doi.org/10.1029/2022GH000711, 2023.

Pusede, S. E., Steiner, A. L., and Cohen, R. C.: Temperature and Recent Trends in the Chemistry of Continental Surface Ozone, Chem. Rev., 115, 3898–3918, https://doi.org/10.1021/cr5006815, 2015.

Reddy, B. S. K., Kumar, K. R., Balakrishnaiah, G., Gopal, K. R., Reddy, R. R., Reddy, L. S. S., Ahammed, Y. N., Narasimhulu, K., Moorthy, K. K., and Babu, S. S.: Potential Source Regions Contributing to Seasonal Variations of Black Carbon Aerosols over Anantapur in Southeast India, Aerosol Air Qual. Res., 12, 344–358, https://doi.org/10.4209/aaqr.2011.10.0159, 2012.

Ren, F., Lin, J., Xu, C., Adeniran, J. A., Wang, J., Martin, R. V., Van Donkelaar, A., Hammer, M., Horowitz, L., Turnock, S. T., Oshima, N., Zhang, J., Bauer, S., Tsigaridis, K., Seland, Ø., Nabat, P., Neubauer, D., Strand, G., Van Noije, T., Le Sager, P., and Takemura, T.: Evaluation of CMIP6 model simulations of $PM_{2.5}$ and its components over China, https://doi.org/10.5194/egusphere-2023-2370, 2023.

Sadavarte, P. and Venkataraman, C.: Trends in multi-pollutant emissions from a technology-linked inventory for India: I. Industry and transport sectors, Atmospheric Environment, 99, 353–364, https://doi.org/10.1016/j.atmosenv.2014.09.081, 2014.

Sahu, L. K., Sheel, V., Pandey, K., Yadav, R., Saxena, P., and Gunthe, S.: Regional biomass burning trends in India: Analysis of satellite fire data, J Earth Syst Sci, 124, 1377–1387, https://doi.org/10.1007/s12040-015-0616-3, 2015.

Saradhi, I. V., Prathibha, P., Hopke, P. K., Pandit, G. G., and Puranik, V. D.: Source Apportionment of Coarse and Fine Particulate Matter at Navi Mumbai, India, Aerosol Air Qual. Res., 8, 423–436, https://doi.org/10.4209/aaqr.2008.07.0027, 2008.

Sarkar, C., Roy, A., Chatterjee, A., Ghosh, S. K., and Raha, S.: Factors controlling the long-term (2009–2015) trend of PM2.5 and black carbon aerosols at eastern Himalaya, India, Science of The Total Environment, 656, 280–296, https://doi.org/10.1016/j.scitotenv.2018.11.367, 2019.

Sen, P. K.: Estimates of the Regression Coefficient Based on Kendall's Tau, Journal of the American Statistical Association, 63, 1379–1389, https://doi.org/10.1080/01621459.1968.10480934, 1968.

Theil, H.: A Rank-Invariant Method of Linear and Polynomial Regression Analysis, in: Henri Theil's Contributions to Economics and Econometrics, vol. 23, edited by: Raj, B. and Koerts, J., Springer Netherlands, Dordrecht, 345–381, https://doi.org/10.1007/978-94-011-2546-8_20, 1992.

Tilmes, S., Lamarque, J.-F., Emmons, L. K., Kinnison, D. E., Ma, P.-L., Liu, X., Ghan, S., Bardeen, C., Arnold, S., Deeter, M., Vitt, F., Ryerson, T., Elkins, J. W., Moore, F., Spackman, J. R., and Val Martin, M.: Description and evaluation of

tropospheric chemistry and aerosols in the Community Earth System Model (CESM1.2), Geoscientific Model Development, 8, 1395–1426, https://doi.org/10.5194/gmd-8-1395-2015, 2015.

Tiwari, S., Srivastava, A. K., Bisht, D. S., Bano, T., Singh, S., Behura, S., Srivastava, M. K., Chate, D. M., and Padmanabhamurty, B.: Black carbon and chemical characteristics of PM10 and PM2.5 at an urban site of North India, J Atmos Chem, 62, 193–209, https://doi.org/10.1007/s10874-010-9148-z, 2009.

Tiwari, S., Srivastava, A. K., Bisht, D. S., Parmita, P., Srivastava, M. K., and Attri, S. D.: Diurnal and seasonal variations of black carbon and $PM_{2.5}$ over New Delhi, India: Influence of meteorology, Atmospheric Research, 125–126, 50–62, https://doi.org/10.1016/j.atmosres.2013.01.011, 2013.

Turner, M. C., Jerrett, M., Pope, C. A., Krewski, D., Gapstur, S. M., Diver, W. R., Beckerman, B. S., Marshall, J. D., Su, J., Crouse, D. L., and Burnett, R. T.: Long-Term Ozone Exposure and Mortality in a Large Prospective Study, Am J Respir Crit Care Med, 193, 1134–1142, https://doi.org/10.1164/rccm.201508-1633OC, 2016.

Turnock, S. T., Allen, R. J., Andrews, M., Bauer, S. E., Deushi, M., Emmons, L., Good, P., Horowitz, L., John, J. G., Michou, M., Nabat, P., Naik, V., Neubauer, D., O'Connor, F. M., Olivié, D., Oshima, N., Schulz, M., Sellar, A., Shim, S., Takemura, T., Tilmes, S., Tsigaridis, K., Wu, T., and Zhang, J.: Historical and future changes in air pollutants from CMIP6 models, Atmospheric Chemistry and Physics, 20, 14547–14579, https://doi.org/10.5194/acp-20-14547-2020, 2020.

Vadrevu, K. P., Lasko, K., Giglio, L., Schroeder, W., Biswas, S., and Justice, C.: Trends in Vegetation fires in South and Southeast Asian Countries, Sci Rep, 9, 7422, https://doi.org/10.1038/s41598-019-43940-x, 2019.

Vanem, E. and Walker, S.-E.: Identifying trends in the ocean wave climate by time series analyses of significant wave heightdata, Ocean Engineering, 61, 148–160, https://doi.org/10.1016/j.oceaneng.2012.12.042, 2013.

Venkatramanan, V., Shah, S., Rai, A. K., and Prasad, R.: Nexus Between Crop Residue Burning, Bioeconomy and Sustainable Development Goals Over North-Western India, Frontiers in Energy Research, 8, 2021.

Villeneuve, P. J., Weichenthal, S. A., Crouse, D., Miller, A. B., To, T., Martin, R. V., van Donkelaar, A., Wall, C., and Burnett, R. T.: Long-term Exposure to Fine Particulate Matter Air Pollution and Mortality Among Canadian Women, Epidemiology, 26, 536, https://doi.org/10.1097/EDE.0000000000000294, 2015.

Vohra, K., Marais, E. A., Bloss, W. J., Schwartz, J., Mickley, L. J., Van Damme, M., Clarisse, L., and Coheur, P.-F.: Rapid rise in premature mortality due to anthropogenic air pollution in fast-growing tropical cities from 2005 to 2018, Science Advances, 8, eabm4435, https://doi.org/10.1126/sciadv.abm4435, 2022.

Wan, L., Bento, V. A., Qu, Y., Qiu, J., Song, H., Zhang, R., Wu, X., Xu, F., Lu, J., and Wang, Q.: Drought characteristics and dominant factors across China: Insights from high-resolution daily SPEI dataset between 1979 and 2018, Science of The Total Environment, 901, 166362, https://doi.org/10.1016/j.scitotenv.2023.166362, 2023.

Wang, H., Lu, X., Jacob, D. J., Cooper, O. R., Chang, K.-L., Li, K., Gao, M., Liu, Y., Sheng, B., Wu, K., Wu, T., Zhang, J., Sauvage, B., Nédélec, P., Blot, R., and Fan, S.: Global tropospheric ozone trends, attributions, and radiative impacts in

1995–2017: an integrated analysis using aircraft (IAGOS) observations, ozonesonde, and multi-decadal chemical model simulations, Atmospheric Chemistry and Physics, 22, 13753–13782, https://doi.org/10.5194/acp-22-13753-2022, 2022.

Wang, L., Zhang, X., and Ming, J.: Aerosol Optical Properties Measured Using a PAX in Central Asia from 2016 to 2019 and the Climatic and Environmental Outlooks, ACS Earth Space Chem., 5, 95–105, https://doi.org/10.1021/acsearthspacechem.0c00306, 2021.

Xie, X., Zhang, Y., Liang, R., Chen, W., Zhang, P., Wang, X., Zhou, Y., Cheng, Y., and Liu, J.: Wintertime Heavy Haze Episodes in Northeast China Driven by Agricultural Fire Emissions, Environ. Sci. Technol. Lett., https://doi.org/10.1021/acs.estlett.3c00940, 2024.

Young, P. J., Naik, V., Fiore, A. M., Gaudel, A., Guo, J., Lin, M. Y., Neu, J. L., Parrish, D. D., Rieder, H. E., Schnell, J. L., Tilmes, S., Wild, O., Zhang, L., Ziemke, J., Brandt, J., Delcloo, A., Doherty, R. M., Geels, C., Hegglin, M. I., Hu, L., Im, U., Kumar, R., Luhar, A., Murray, L., Plummer, D., Rodriguez, J., Saiz-Lopez, A., Schultz, M. G., Woodhouse, M. T., and Zeng, G.: Tropospheric Ozone Assessment Report: Assessment of global-scale model performance for global and regional ozone distributions, variability, and trends, Elementa: Science of the Anthropocene, 6, 10, https://doi.org/10.1525/elementa.265, 2018.

Yue, M., Dong, X., Wang, M., Emmons, L. K., Liang, Y., Tong, D., Liu, Y., and Liu, Y.: Modeling the Air Pollution and Aerosol-PBL Interactions Over China Using a Variable-Resolution Global Model, JGR Atmospheres, 128, e2023JD039130, https://doi.org/10.1029/2023JD039130, 2023.

Zhang, R., Wu, X., Zhou, X., Ren, B., Zeng, J., and Wang, Q.: Investigating the effect of improved drought events extraction method on spatiotemporal characteristics of drought, Theor Appl Climatol, 147, 395–408, https://doi.org/10.1007/s00704-021-03838-z, 2022a.

Zhang, R., Qi, J., Leng, S., and Wang, Q.: Long-Term Vegetation Phenology Changes and Responses to Preseason Temperature and Precipitation in Northern China, Remote Sensing, 14, 1396, https://doi.org/10.3390/rs14061396, 2022b.

Zhang, Y., Cooper, O. R., Gaudel, A., Thompson, A. M., Nédélec, P., Ogino, S.-Y., and West, J. J.: Tropospheric ozone change from 1980 to 2010 dominated by equatorward redistribution of emissions, Nature Geosci, 9, 875–879, https://doi.org/10.1038/ngeo2827, 2016.

Zhang, Y., West, J. J., Emmons, L. K., Flemming, J., Jonson, J. E., Lund, M. T., Sekiya, T., Sudo, K., Gaudel, A., Chang, K.-L., Nédélec, P., and Thouret, V.: Contributions of World Regions to the Global Tropospheric Ozone Burden Change From 1980 to 2010, Geophysical Research Letters, 48, e2020GL089184, https://doi.org/10.1029/2020GL089184, 2021a.

Zhang, Y., Shindell, D., Seltzer, K., Shen, L., Lamarque, J.-F., Zhang, Q., Zheng, B., Xing, J., Jiang, Z., and Zhang, L.: Impacts of emission changes in China from 2010 to 2017 on domestic and intercontinental air quality and health effect, Atmos. Chem. Phys., 21, 16051–16065, https://doi.org/10.5194/acp-21-16051-2021, 2021b.

Zhou, H., Zhou, C., Lynam, M. M., Dvonch, J. T., Barres, J. A., Hopke, P. K., Cohen, M., and Holsen, T. M.: Atmospheric Mercury Temporal Trends in the Northeastern United States from 1992 to 2014: Are Measured Concentrations

Responding to Decreasing Regional Emissions?, Environ. Sci. Technol. Lett., 4, 91–97, https://doi.org/10.1021/acs.estlett.6b00452, 2017.